fire

MDPI

Article

Effect of Perchlorate on Combustion Properties of Directly-Written Al/PVDF Composites

Jingwei Li [1,2,†], Xuwen Liu [1,2,†], Quanmin Xie [1], Jiaxin Su [2], Maocong Hu [1,3,*] and Zhenhua Yao [1,3,*]

[1] State Key Laboratory of Precision Blasting, Jianghan University, Wuhan 430056, China
[2] School of Chemistry and Chemical Engineering, Nanjing University of Science and Technology, Nanjing 210094, China
[3] School of Optoelectronic Materials & Technology, Jianghan University, Wuhan 430056, China
* Correspondence: maocong.hu@jhun.edu.cn (M.H.); zhenhua.yao@jhun.edu.cn (Z.Y.); Tel.: +86-189-7112-8395 (M.H.); +86-189-9553-3486 (Z.Y.)
† These authors contributed equally to this work.

Abstract: Metastable intermolecular composites (MICs) based on Al/PVDF have become one of the most important materials in the field of additive manufacturing of energetic materials due to their high energy density and designability. In this work, the energy utilization efficiency and energy release performance of directly written Al/PVDF composites were regulated by introducing ammonium perchlorate (AP) and potassium perchlorate (KP) as gas generators and oxidants. The effect of AP/KP on the combustion performance of MICs systems has been studied in depth. It was found that the addition of AP/KP can increase the combustion temperature and flame duration of the Al/PVDF system. Moreover, the flame propagation rate of the Al/PVDF system decreases as AP/KP addition increases. Therefore, the strategy of introducing AP/KP into directly written Al/PVDF composites can effectively control the energy performance of this energetic system, thereby promoting its practical application in propellants, heterogeneous explosives and gas generators.

Keywords: metastable intermolecular composite; n-Al/PVDF; perchlorate; direct ink writing; combustion properties

Citation: Li, J.; Liu, X.; Xie, Q.; Su, J.; Hu, M.; Yao, Z. Effect of Perchlorate on Combustion Properties of Directly-Written Al/PVDF Composites. *Fire* **2023**, *6*, 106. https://doi.org/10.3390/fire6030106

Academic Editors: Clive Woodley and Grant Williamson

Received: 31 January 2023
Revised: 24 February 2023
Accepted: 6 March 2023
Published: 8 March 2023

1. Introduction

Energetic materials are substances that can undergo redox reactions and release a large amount of energy under certain external stimuli. Examples include explosives, propellants and pyrotechnic agents [1]. These materials are all compounds or mixtures containing explosive groups or containing oxidants and combustibles, which can independently carry out chemical reactions and release energy [2]. Nanothermites, also known as metastable interstitial composites, are composed of a nanoscale oxidizing agent and a nanoscale reducing agent [3]. Nanothermites are the future development trend. Compared with a traditional thermite, the specific surface area of nanothermite components is significantly increased, and the oxidizing agent and reducing agent are in close contact, which enhances the reactivity of the entire energetic system, causing the rate of energy release to increase rapidly [4]. The excellent properties of nanothermites make them very promising in the field of ignition and detonation, and they have become a hot spot in the field of energetic materials research [5].

Currently, aluminum is the most widely studied metal fuel in metastable interstitial composites because of its high energy density and easy availability [6]. However, during the oxidation process, aluminum and its oxides tend to condense to form larger aggregates, resulting in the loss of two-phase flow, thus limiting the energy release of the system [7,8]. In addition, the nanoscale thermite composition also has low electrostatic safety issues, which limit its development in applications [9]. In recent years, it has been considered that

fluorine can effectively react with aluminum to effectively alleviate the above-mentioned disadvantages [6,10].

Compared with the traditional Al-O reaction in Al-based energetic systems, the Al-F reaction has unique advantages, which have attracted the interest of a large number of researchers [11–13]. On the one hand, because fluorine has a higher electronegativity than oxygen, fluorochemicals can undergo a pre-ignition reaction with the alumina shell before the ignition temperature [14], improving the energy efficiency utilization of the system and promoting the release of aluminum energy. On the other hand, the heat of formation of the Al-F reaction is equivalent to that of the Al-O reaction (the heat of formation of Al_2O_3 is 55.67 kJ/g, and the heat of formation of AlF_3 is 30.96 kJ/g) [15].

Therefore, researchers have shown much interest in the metal/fluoride composition of energy systems with favorable energy properties. Mg/PTFE/Viton (MTV) compositions are widely used in research related to infrared decoys due to their excellent infrared radiation ability during combustion [16,17]. Al/PTFE compositions have high energy-release capabilities under dynamic loads [18,19]. Al/THV is considered to be a good propellant additive [20]. As for the Al/PVDF composition, due to its integrated good reactivity and flexible processability capabilities, it has a wide range of application prospects and has attracted extensive interest from researchers [21].

The Al/PVDF composite has a higher energy density (947.7 kJ compared to 600 kJ per mol for Al) than conventional Al/CuO [21]. PVDF releases HF during the reaction with Al, while fluorination of the inert Al_2O_3 shell releases energy components and exposes fresh Al [15]. Moreover, the good mechanical and film-forming properties of PVDF enable Al/PVDF to have the characteristics of flexible processing [22]. Compared with traditional powder-shaped energetic materials, the Al/PVDF system has better integration and can be applied in advanced manufacturing. For traditional powdery energetic materials, the processing is often cumbersome and difficult, and sometimes accompanied by potential safety hazards [9]. Currently in the field of energetic materials, miniaturization of pyrotechnic devices, precise charging, flexible charging and intelligent charging are required [23]. However, in many application scenarios, powdery energetic materials have disadvantages in terms of design capability and integration [24]. Therefore, researchers have attempted to prepare reactive-based thin films using electrodeposition or magnetron sputtering techniques [25,26]. Alternatively, energetic inks have been formulated by adding a binder to a powdered thermite [27]. Based on these ideas, the researchers explored various processes for forming shapes from energetic material powders. Due to the advantages of simple manufacturing process, rapidity and low cost, direct ink writing technology can be combined with 3D printing technology to realize the integration of reactive materials in complex three-dimensional structures [23,28,29]. In addition, it enables precise charging of energetic materials. The energy-release properties of reactive materials formed by direct writing can also be altered by printing thickness [15]. Therefore, the Al/PVDF system based on direct ink writing is compatible with advanced manufacturing and has attracted extensive attention from researchers.

In recent decades, a variety of Al/PVDF-based composites have been developed using various methods, such as microfluidic synthesis [21], direct ink writing [15], inkjet printing [30], electrospray deposition [31,32], electrospinning [33], ice template [14] and modified microemulsion synthesis [34]. Most of the research focuses on the functionalization of Al/PVDF materials by various means to expand their application potential.

However, for the combustion reaction between PVDF and Al, the product contains H_2 and a large amount of carbon, which causes the energy generated by the system reaction to not be fully utilized [21]. To resolve to this problem, adding mixed oxidants into the Al/PVDF system has become a feasible path. As part of the research related to the addition of oxidants to Al/PVDF, Zachariah [35] has studied the performance changes when metal oxides are added to the Al/PVDF system. In the studies in Zachariah and the report on those studies, it is shown that the introduction of additional oxidizers can slow down the reaction rate of the Al/PVDF system and increase its temperature during the combustion

process. The introduction of additional oxidants is an effective way to adjust the output energy of the Al/PVDF system.

In the field of energetic materials research, perchlorate has been proven to be an oxidant that can effectively increase the surface temperature of nanoparticles in the reaction system, thereby improving its combustion effect. Therefore, this work attempts to add oxidants AP and KP to the Al/PVDF system at the stoichiometric ratio $\Phi = 1$. AP and KP are used as gas generators and oxidants to improve the energy output efficiency of the system. High-speed photography and a spectrophotometer are utilized to study the reactivity characteristics of the Al/PVDF system after adding AP and KP, and more importantly, the change in combustion temperature and its mechanism.

2. Materials and Methods

2.1. Materials

Al nanopowder (Al NPs, with an average particle size of 70 nm) was purchased from Shanghai BAK New Material Technology Co., Ltd (Shanghai, China). By calcining the Al NPs in air, the active Al content was calculated to be about 72%, as shown in Table 1. PVDF (Mw of 250,000–500,000) was purchased from Shanghai McLean Biochemical Technology Co., Ltd. (Shanghai, China). Anhydrous ethanol and N,N-dimethylformamide (DMF, 99.8%), Ammonium perchlorate (AP) and potassium perchlorate (KP) were purchased from Sinopharm Chemical Reagent Co., Ltd. (Shanghai, China).

Table 1. Results of activity measurement of Al NPs.

Serial	Before Calcination (mg)	After Calcination (mg)	Active Aluminum Content (%)
1	240	392	71.3
2	245	403	72.5
3	240	393	71.7
4	243	401	73.1
5	241	397	72.8

2.2. Preparation of Energetic Inks

In the process of preparing the high-energy ink, PVDF was first added to DMF and magnetically stirred for 12 h to form a uniform transparent solution. Next, the Al NPs and the AP or KP were put into the PVDF/DMF solution for 30 min and then stirred for 10 h to ensure their uniform dispersal in the solution. The chemical composition of each prepared mixture is listed in Table 2.

Table 2. Chemical composition.

Formulation	Al NPs (mg)	PVDF (mg)	AP (mg)	KP (mg)	DMF (mL)
AP	214	500	0	0	5
APA-3	214	479	21	0	5
APA-6	214	458	42	0	5
APA-9	214	437	63	0	5
APK-3	214	479	0	21	5
APK-6	214	458	0	42	5
APK-9	214	437	0	63	5

Then, the prepared inks were written using a pneumatic injector (Figure 1). The feed rate was ~5 mL/h and the needle size was ~0.8 mm. The stage bonded to the substrate was heated to ~80 °C prior to printing to allow the solvent to evaporate before printing subsequent layers.

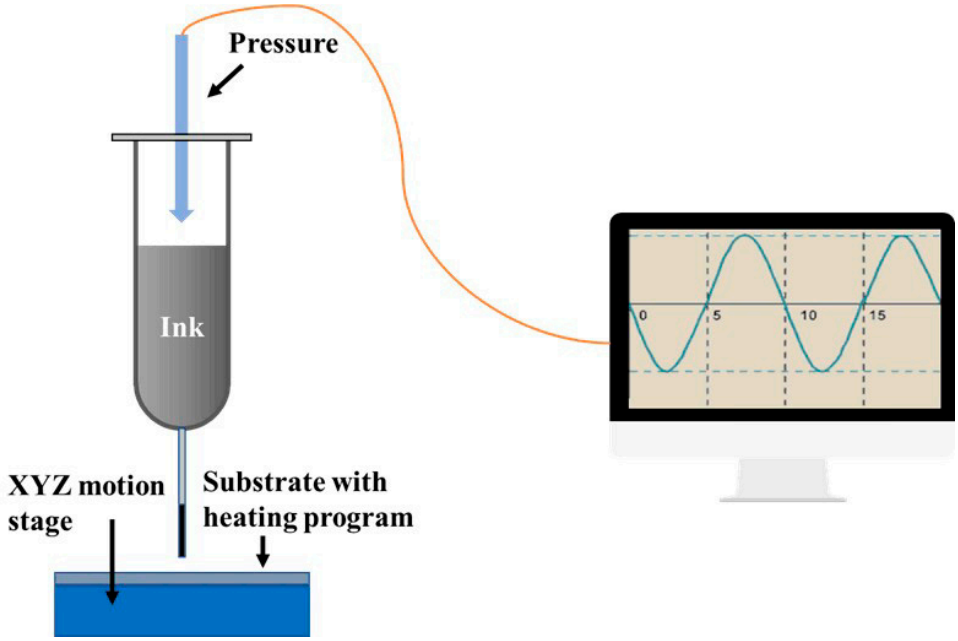

Figure 1. Schematic illustration of the direct writing method with energetic inks using a pneumatic injector.

2.3. Characterization and Performance Test

The morphologies of the samples were characterized by field-emission scanning electron microscope (SEM, FEI, Quanta 250F). The elemental analysis of was performed by energy dispersive spectrometry (EDS). The flame propagation process under open conditions was studied using a high-speed camera (Phontron FASTCAM Mini UX100). On a glass substrate, the inks were printed in stripes with a length of about 50 mm and a line width of about 3.5 mm. The ignition behavior of energetic inks was studied using a Nichrome wire ignition device. The resistance of the nickel-chromium bridge wire igniter used in this study was 0.7~0.9Ω. The sample mass of the igniter was 50 ± 1.3 mg. When the nickel-chromium bridge wire igniter was used to test the ink burning, the external stimulation energy was provided by 20 V and 10A DC power supply. The emission spectrum information of the flame was measured by a spectrophotometer (Beijing Normal University Instrument Factory).

3. Results

3.1. Morphology

Figure 2 shows the SEM images of the original n-Al/PVDF system and the n-Al/PVDF system sample surface after adding an oxidant (ammonium perchlorate). As shown in Figure 2a,c, the surface of the pristine n-Al/PVDF sample is relatively smooth and dense, no large numbers of wrinkles are observed, and there are many protrusions and micropores [14,15]. The micropores may be formed by the solvent after evaporation. The Al NPs inside the sample are embedded in PVDF, and the interface between the two is relatively tight. Coating polymers to limit oxygen diffusion is considered an effective way to avoid further oxidation of reactive metals in air [14]. Therefore, the structure of Al NPs embedded in PVDF matrix is beneficial to the maintenance of the anti-aging ability of the system. As shown in Figures 2b,d and 3a,b, with the addition of AP and KP, fine wrinkles began to appear on the sample surface. This is mainly due to the shape change caused by the crystallization of AP and KP when the solvent evaporates to form the sample. From the SEM characterization, it can be seen that, on the microscopic scale, the addition of AP and KP can directly affect the morphology of the APA(K) system through the crystallization process. Figure 3c,d show the distribution of Al, C, Cl and F elements in the samples. Among them, C and F elements represent PVDF, Al elements represent Al NPs and Cl elements

represent AP. All elements are evenly distributed, indicating that these components are well dispersed in the sample.

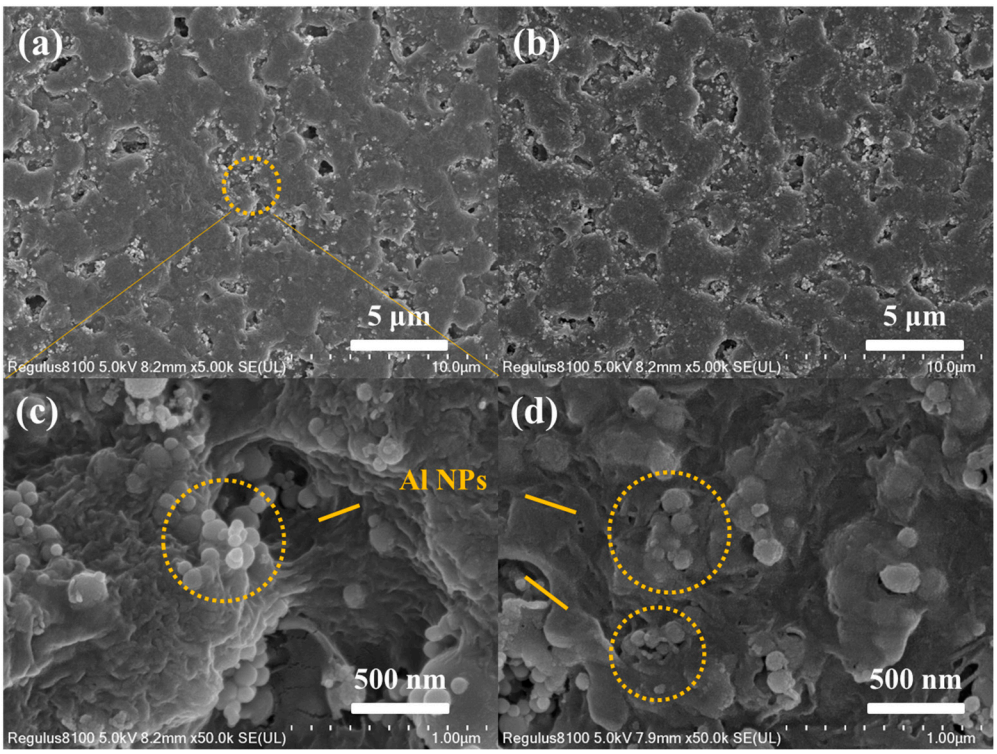

Figure 2. Top-view SEM images at different magnifications of (**a**,**c**) AP, (**b**,**d**) APA-6.

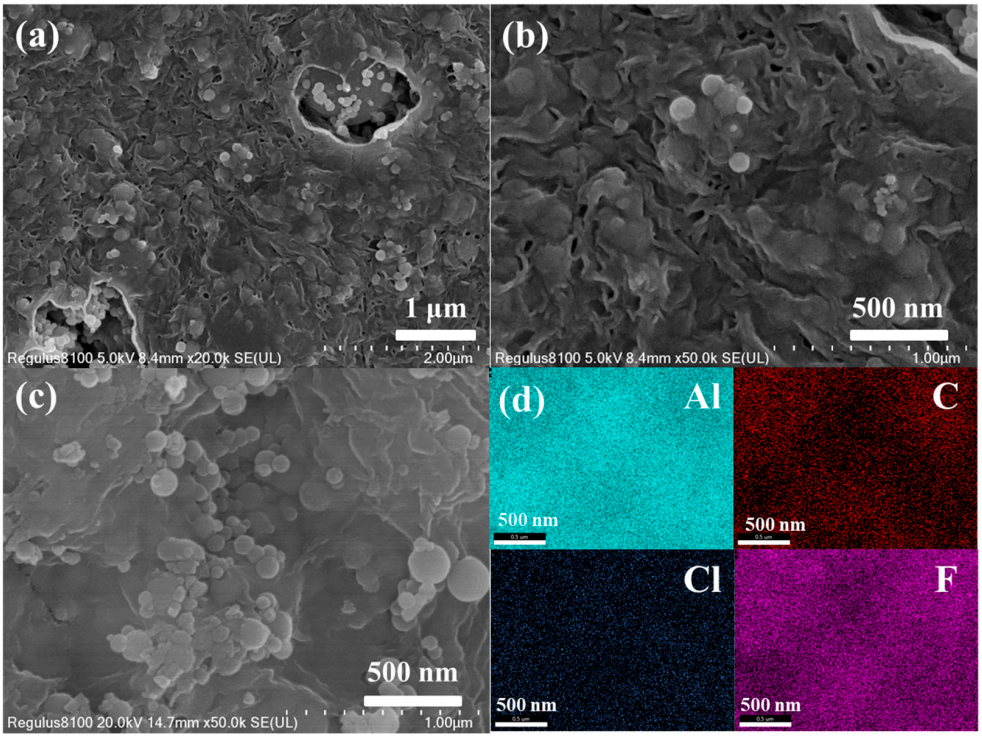

Figure 3. (**a**,**b**) Top-view SEM images at different magnifications and (**c**,**d**) elemental mapping images of Al, C, Cl and F species of APK-3.

3.2. Flame Propagation under Open Conditions

Flame propagation velocity is an important parameter of direct ink writing of energetic materials, reflecting the energy-release rate of the system. To measure the rate of flame spread of each sample under open conditions, individual strips of the sample (50 mm long and 3.5 mm wide) were printed and placed on a quartz plate, ignited by a nickel-chromium wire. Figure 4 shows a typical sequence of snapshots and the average flame-spread rate of the sample combustion process. Each sample can undergo a self-propagating reaction in air after being ignited. For the n-Al/PVDF flame in air, the color rapidly changes from bright white to dark orange as gas products and ejected particles move from the substrate to the open peripheral area. This is mainly because, for the n-Al/PVDF system, the main heterogeneous exothermic reaction occurs between n-Al and small fluorine-containing molecules decomposed by PVDF (such as CF_x, $C_xH_yF_z$ and HF) [15,35]. The reaction product contains a large amount of low-boiling AlF_3 (1537 °C), rather than the Al oxidation product Al_2O_3. Therefore, the radiation characteristics of its flame are different from the n-Al-based energetic system mainly composed of Al_2O_3 products.

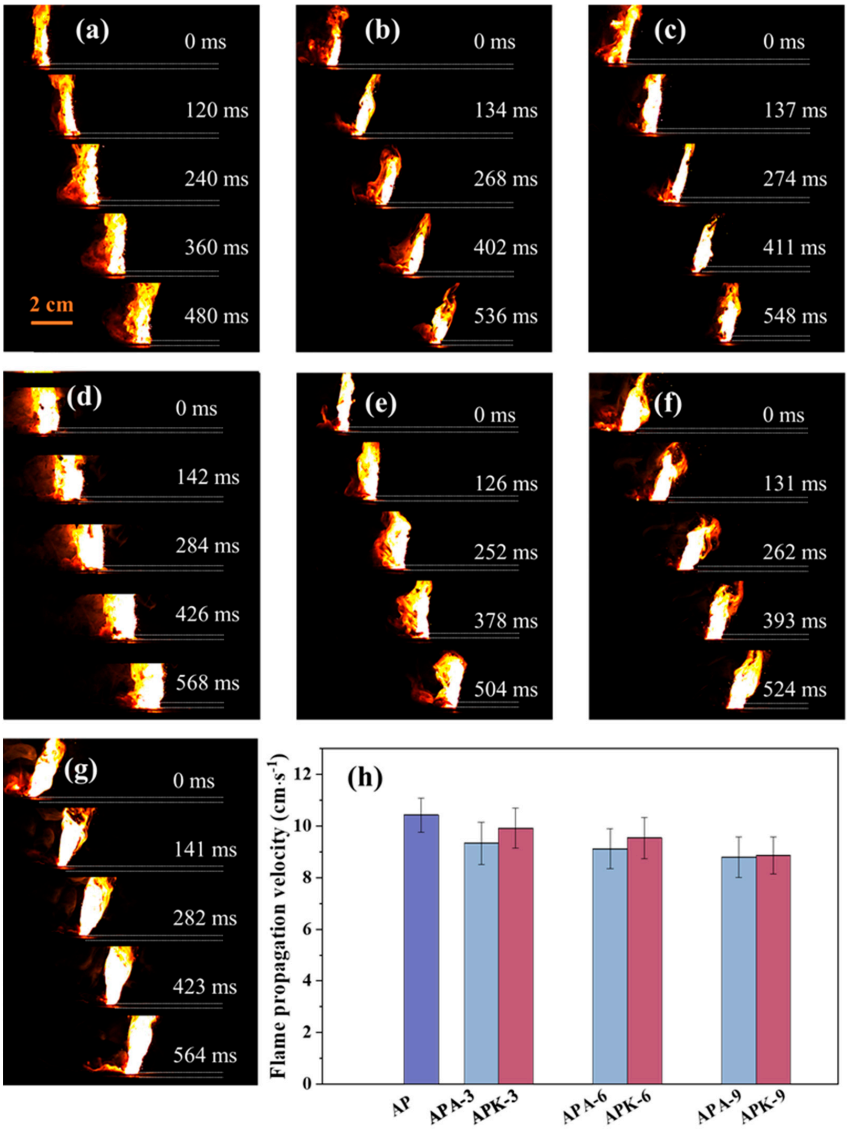

Figure 4. Flame propagation velocity of each sample under open conditions: (**a**) AP, (**b**) APA-3, (**c**) APA-6, (**d**) APA-9, (**e**) APK-3, (**f**) APA-6, (**g**) APA-9. (**h**) Average flame propagation velocity of each sample.

Whether AP is added or KP is added, the flame propagation rate of the n-Al/PVDF system decreases to varying degrees, as shown in Figure 4h. When the AP content in the system increased to 9%, the flame propagation velocity of the n-Al/PVDF system decreased from 10.42 ± 0.77 cm·s^{-1} to 9.33 ± 0.82 cm·s^{-1}, 9.12 ± 0.78 cm·s^{-1} and 8.80 ± 0.79 cm·s^{-1}. When the KP content increased to 9%, the flame propagation velocity of the n-Al/PVDF system decreased from 10.42 ± 0.77 cm·s^{-1} to 9.92 ± 0.76 cm·s^{-1}, 9.54 ± 0.80 cm·s^{-1} and 8.86 ± 0.71 cm·s^{-1}. Zachariah et al. found that when metal oxidants were added to the n-Al/PVDF system, the flame propagation rate of the system decreased significantly [35]. The possible mechanism given in the study is that the Al fluorination reaction is the main reaction driving the n-Al/PVDF-based flame propagation, and the reaction between the additional oxidants and Al in the system occurs behind the flame front. This is consistent with the phenomenon seen in this study: the addition of oxidants slows down the reaction of the system. Moreover, with the addition of AP/KP, the bright white part of the flame is greatly increased. This may be because the formation of more Al_2O_3 in the combustion products changes the radiative properties of the flame as the oxidant content increases.

3.3. Flame Temperature

Flame emission spectrum analysis is an important method for analyzing the characteristics of the combustion process. The detected typical emission spectrum results are shown in Figure 5, and all samples exhibit typical blackbody radiation characteristics. The emission peak at ~760 nm is the atomic emission peak of the K element [36,37]. In the study of combustion emission characteristics of energetic substances, even if there is no K element in the system, the emission peak of impurity K atoms is often unavoidably detected [36,37]. In the n-Al/PVDF system with KP added, the emission peak of K atoms comes from the decomposition of potassium perchlorate in the combustion process. For the n-Al/PVDF system with AP added, the emission peak of K atoms also comes from the K impurity in the system. With the increase in AP/KP content, the emission peak of K atoms is also enhanced.

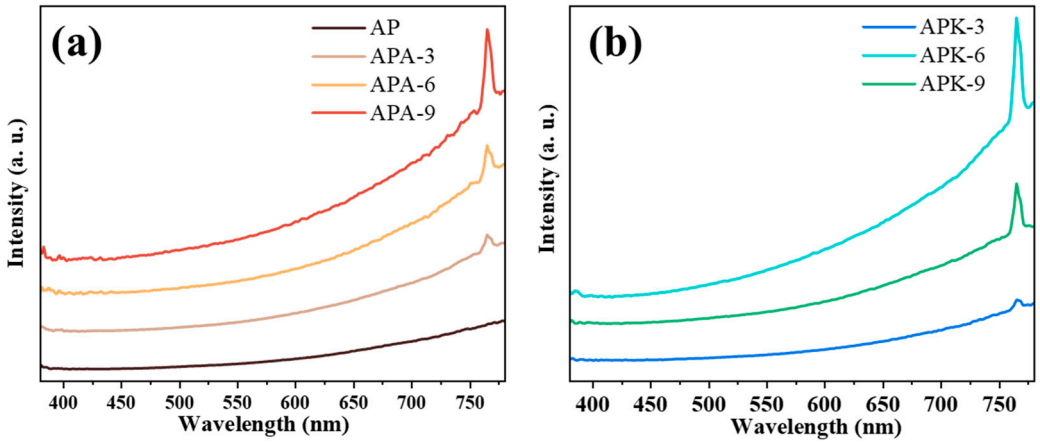

Figure 5. Typical combustion spectra of the samples: (**a**) AP, APA-3, APA-6, APA-9; (**b**) APK-3, APA-6, APA-9.

The calculation of the combustion temperature is realized by analyzing the emission spectrum by using the multi-wavelength pyrometer theory [38]. Following Planck's law, Equation (1) gives the thermal radiation emission intensity, where λ is the wavelength, T is the temperature and ε is the emissivity. c_1 and c_2 are well known Planck's constants. For real object surfaces, the emissivity is not constant.

$$E(T,\lambda) = \varepsilon \cdot \frac{c_1}{\lambda^5[\exp(C_2/T\lambda)-1]} \quad (1)$$

For n-Al-based energetic materials, the temperature is usually calculated by assuming a functional dependence of the emissivity ($\varepsilon \sim \lambda^{-1}$ and independent of temperature) during the calculation, as shown in Equation (2). Equation (3) is obtained by taking the natural logarithm on both sides of Equation (1). The quantity Z is defined by Equation (4). The temperature is then determined from the slope, using a plot of Z versus the reciprocal wavelength, as shown in Figure 6a.

$$\varepsilon(\lambda) = \frac{c_3}{\lambda} \tag{2}$$

$$\ln\left(\varepsilon(\lambda, T) \cdot \frac{c_1}{\lambda^5} \cdot [E(T, \lambda)]^{-1}\right) = \frac{c_2}{\lambda T} \tag{3}$$

$$Z = \ln\left(\frac{c_1}{\lambda^6} \cdot [E(T, \lambda)]^{-1}\right) = \frac{c_2}{\lambda T} - \ln(c_3) \tag{4}$$

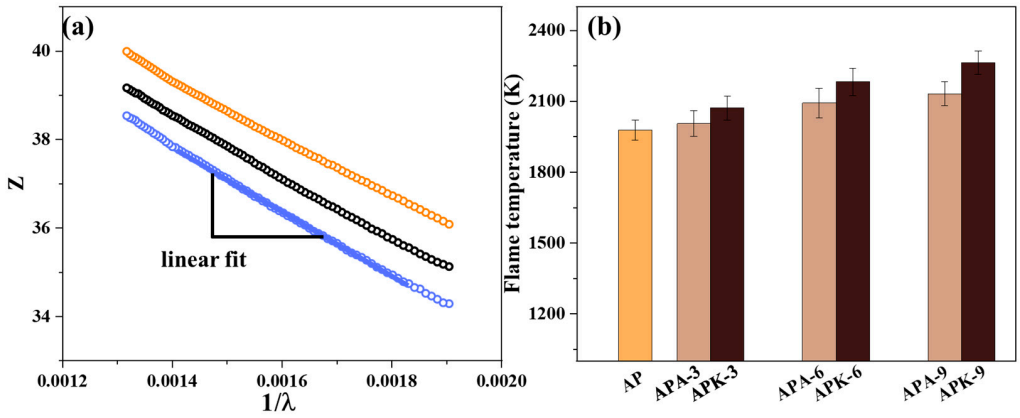

Figure 6. (**a**) The linear fitting curve of the combustion emission spectrum and (**b**) the average combustion temperature of each sample.

Figure 6b shows the average temperature calculated for each sample. Regardless of whether AP or KP is added, the flame temperature of the n-Al/PVDF system increases to varying degrees, as shown in Figure 4h. When the AP content in the system increases to 9%, the flame temperature of the n-Al/PVDF system increases from 1978 ± 42 K to 2006 ± 54 K, 2093 ± 62 K and 2132 ± 51 K. When the KP content increased to 9%, the flame propagation velocity of the n-Al/PVDF system increased from 1978 ± 42 K to 2072 ± 51 K, 2183 ± 58 K and 2263 ± 49 K. This is also consistent with the trend in literature [35], that is, after adding an oxidant to the n-Al/PVDF system, the flame temperature of the system increases significantly during combustion. This shows that the addition of AP/KP can effectively increase the temperature of the system flame. This is consistent with the results in Section 3.2 above: as the AP/KP content increases, the bright white part of the flame increases, which means that the flame has a higher temperature. This also means that by adjusting the AP/KP content, the energy output of the n-Al/PVDF system can be effectively controlled.

3.4. Ignition Performance of Energetic Systems

When the nickel-chromium wire igniter is used to test the ignition performance, the input energy is provided by a constant current source. Ink samples were printed on Ni-Cr bridges, about 50 mg per sample. Among the samples investigated here, all the samples could be successfully ignited by the Ni-Cr wire igniter with a bright flame, as shown in Figure 7. The nickel-chromium bridge wire on the Ni-Cr igniter melts under the heat of the current, thereby transferring heat to the energetic system along the nickel-chromium wire. Similar to the phenomenon seen in Section 3.2, the center part of the flame of the pure n-Al/PVDF system is bright white, and the edge is dark orange–yellow. As shown in

Figure 7, the burning flame of AP is orange–yellow as a whole, and the bright white part in the center is relatively small. Moreover, when the addition of perchlorate reached 6% or 9% (APA-6, APA-9, APK-6 and APK-9), the flame shows a large bright-white area. This indicates that the addition of AP/KP changes the radiation characteristics of the flame and increases the flame temperature, as described in Section 3.3.

Figure 7. Ignition performance test of various samples on Nichrome wire igniter.

Figure 8 shows the continuous burning time of each sample on the Ni-Cr igniter. When the AP content in the system increased to 9%, the burning time increased from 456 ± 43 ms to 498 ± 52 ms, 521 ± 46 ms and 539 ± 41 ms. When the KP content increased to 9%, the flame duration of the n-Al/PVDF system increased from 456 ± 43 ms to 478 ± 42 ms, 496 ± 49 ms and 536 ± 52 ms. The prolongation of the flame duration on the Ni-Cr igniter may be due to the fact that the reaction rate of the system is determined by the Al-F reaction, and the reaction between perchlorate and Al occurs behind the flame front. Therefore, the addition of perchlorate prolongs the burning time of the flame. This shows that the addition of perchlorate can effectively improve the energy output of the n-Al/PVDF system.

The ignition energy is calculated by the formula $E = \int_0^t UIdt$, where U is the voltage, I is the current and t is the ignition delay time. Since a large part of the input energy is used to heat the nickel-chromium wire, it will not be transferred to the sample. Therefore, the normalized ignition energy was used as a scalar in this study. Figure 9 shows the ignition delay versus normalized ignition energy for each sample. In the Al/PVDF system, with the addition of perchlorate, the ignition delay and normalized ignition energy were both significantly increased. The maximum value was reached at 9% perchlorate addition, increasing from 0.782 ± 0.032 s and 24.08 ± 1.06 J for AP to 0.852 ± 0.038 and 27.01 ± 1.25 (APA-9), and 0.872 ± 0.033 and 27.46 ± 1.51 (APK-9). This shows that the addition of perchlorate will increase the ignition threshold of the Al/PVDF system. This is consistent with the conclusion reached in Section 3.2, that is, that the energy output rate of the Al/PVDF

system is dominated by the Al-F reaction. Since fluorine has a higher electronegativity than O, a large number of researchers have found that PVDF can undergo a pre-ignition reaction with Al before the ignition temperature to improve the ignition performance of the system. It is therefore speculated that the addition of perchlorate weakens the Al-F reaction process when the system is ignited. Thus, the addition of perchlorate will increase the ignition threshold of the Al/PVDF system.

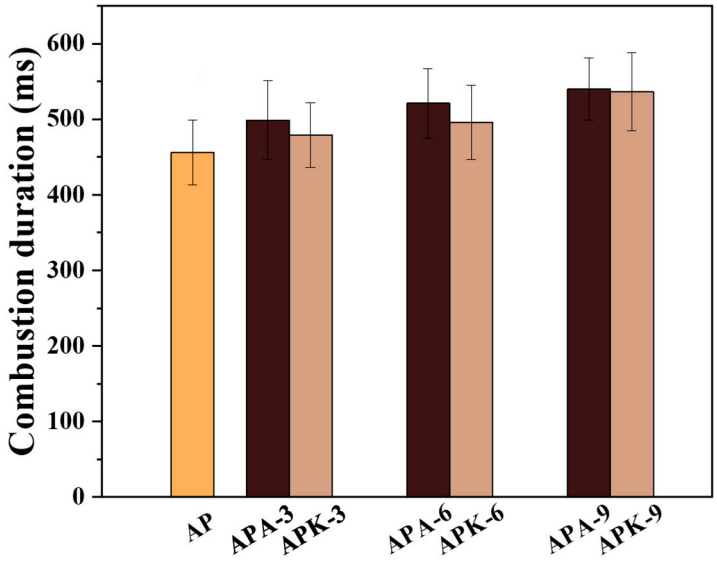

Figure 8. Continuous burning time of each sample on Ni-Cr wire igniter.

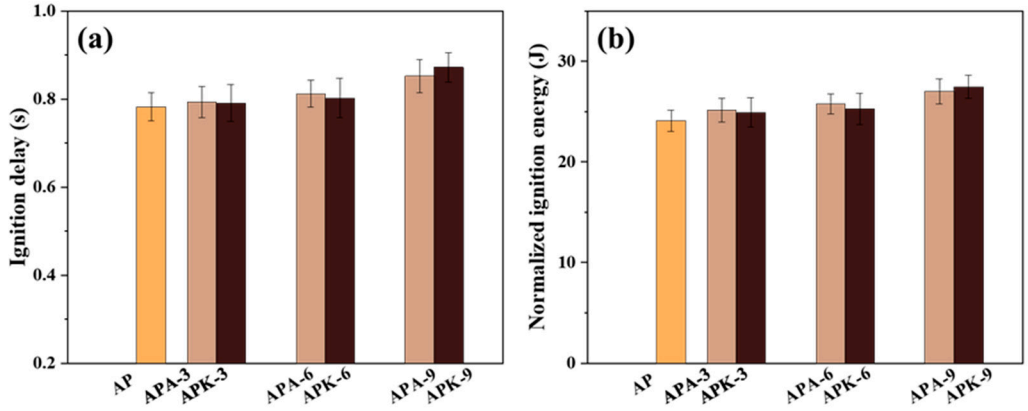

Figure 9. Ignition delay (**a**) and normalized ignition energy (**b**) for each sample.

4. Discussion

As a polymer, PVDF will form a complex three-dimensional nanostructure when it is compounded with aluminum micro-nanoscale particles. This leads to complex heterogeneous processes involving heat conduction, heat convection and heat radiation when the Al/PVDF composite system undergoes self-propagating combustion. In addition, the multivariate chemical reaction process is also an interesting feature in the reaction process of such energetic systems. Because PVDF is an fluorine -containing polymer, both its O element and its F element will chemically react with Al, leading to the existence of two routes, namely Al-O and Al-F, in the exothermic process. At present, although the quantitative characterization of these two pathways is still lacking, researchers have done a lot of work to gain a deep understanding of the Al/PVDF reaction process. When the reaction occurs in different atmospheres, the products formed are different, so it can be deduced that there are differences in the reaction pathways. For the Al/PVDF energetic system prepared

using the electrospray method, when it undergoes self-sustained combustion in argon, the product formed after combustion is mainly AlF_3. Interestingly, when this reaction takes place in air, different main combustion products (Al_2O_3 and Al_4C_3) are produced [39]. In addition to the reaction atmosphere, it seems that the microscopic morphology of the material and the preparation method also have an impact on the reaction pathway of such systems. The reaction products of Al/PVDF energetic systems prepared by freeze-drying and additive manufacturing are somewhat different from those of systems which use sponge-like Al/PVDF films [14,21,40,41].

Figure 10a,b show the SEM images of the combustion products of the n-Al/PVDF system. The combustion products are mainly convoluted layered carbon, inlaid with granular products of aluminum combustion. Figure 10c shows the XRD images of the combustion products of the n-Al/PVDF system before and after adding oxidants. Among them, the diffraction peaks of 45.7° and 66.9° belong to Al_2O_3 (JCPDs No.46-1131). The results of Al 2p fine spectrum by XPS show that Al-O (74.6 eV) and Al-F (76.6 eV) exist in each sample, as shown in Figure 10d–f. The difference is that the peak area ratio of Al-O relative to Al-F increases after adding oxidants. As shown in Figure 10d–f, the peak area ratio of Al-O/Al-F in the AP system is 8.06, while the peak area ratios of Al-O/Al-F in the APA-6 and APK-6 systems are 9.21 and 12.08. This indicates that the addition of perchlorate can enhance the Al-O reaction in the n-Al/PVDF system. This also partly justifies the reasons for the changes in the experimental phenomena described in the previous sections, including the flame radiation characteristics, flame temperature and energy release rate.

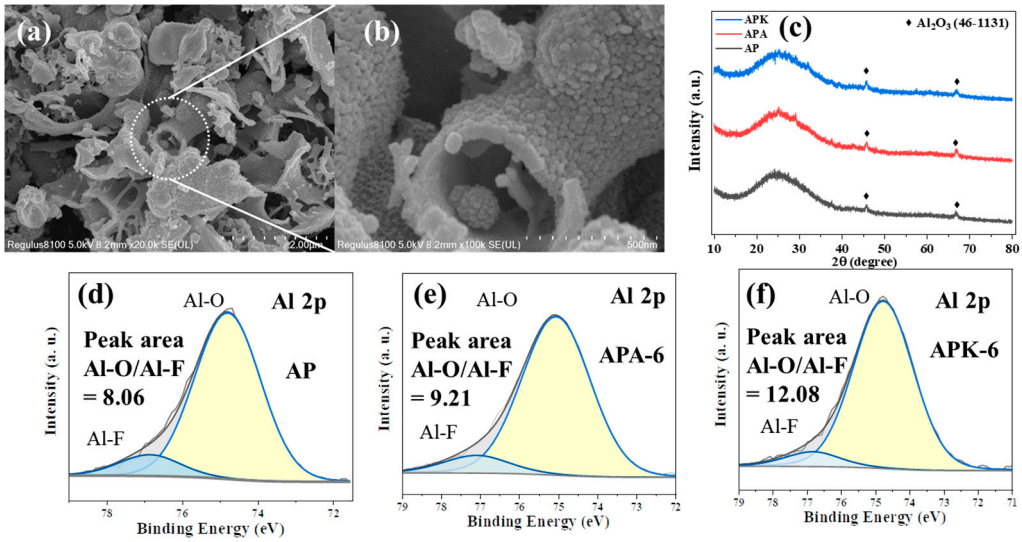

Figure 10. SEM images (**a**,**b**) and XRD images (**c**) of n-Al/PVDF combustion products; Al 2p XPS refined spectra of combustion products of samples AP (**d**), APA-6 (**e**) and APK-6 (**f**).

From the above discussion, it can be seen that research on the Al/PVDF reaction path is currently a challenging topic. This is not only because of the intersecting and multistep chemical reaction pathways, but also because of the extremely complex three-dimensional micro-nanostructure caused by the inherent adjustable and designable morphology of Al/PVDF [14,21]. These factors work together to create a complex reaction environment. To obtain a further understanding of the combustion mechanism of the Al/PVDF system, it is not enough to observe and characterize the combustion process, but also to analyze the combustion products. In this work, the combustion process of Al/PVDF films before and after adding AP/KP was investigated, and the relationship between Al-O and Al-F reactions was explored by product analysis. As an active material that is highly prone to oxidation, Al often has an Al_2O_3 shell on its surface. For Al/PVDF, the advantage of this reaction system is that PVDF can undergo a surface pre-ignition reaction with Al_2O_3 as the

shell layer. After the pre-ignition reaction, the Al_2O_3 shell is destroyed, exposing fresh Al as the nucleus. At this stage, the main, competing Al-O and Al-F reactions occur.

For this work, the research focus was on the energy characteristics of the Al/PVDF system before and after adding AP/KP. In order to gain a deep understanding of the system's energy characteristics, its flame propagation rate, combustion radiation characteristics, combustion temperature and effect on the energy release performance of Ni-Cr igniters under open conditions were investigated. In addition, through the analysis of combustion products, the reaction path of the combustion process of the composite energetic system after addition of AP/KP was studied.

5. Conclusions

The effect of perchlorate (AP/KP) on combustion properties of directly written n-Al/PVDF composites is systematically discussed in this paper. Adding AP or adding KP causes the flame propagation rate of the n-Al/PVDF system to decrease to different degrees. This indicates that the addition of oxidants slows down the reaction of the system. Moreover, with the addition of AP/KP, the bright white part of the flame produced by the combustion of the energetic system greatly increases. This may be due to the formation of more Al_2O_3 in the combustion products as the oxidant content increases, thus changing the radiative properties of the flame. The addition of soluble perchlorate also increases the temperature of the flame generated by the combustion of directly written n-Al/PVDF composites. One possible mechanism for this phenomenon is that AP/KP can effectively increase the surface temperature of nanoparticles in the reaction system. In addition, AP/KP increases the continuous burning time of n-Al/PVDF composites on a Ni-Cr igniter. Therefore, adding AP/KP to the MICs system can adjust its burning rate, burning temperature and burning duration, thus providing a technical path for designing directly written n-Al/PVDF composites suitable for different application scenarios, and promoting their practical application in the field of advanced pyrotechnics.

Author Contributions: Conceptualization, J.L. and X.L.; Data curation, J.L.; Formal analysis, J.L. and Q.X.; Investigation, J.S.; Methodology, J.L. and Q.X.; Project administration, X.L.; Resources, M.H. and Z.Y.; Software, X.L. and Z.Y.; Supervision, M.H. and Z.Y.; Validation, J.S.; Visualization, J.L.; Writing—original draft, J.L. and M.H.; Writing—review and editing, J.L. and X.L. All authors have read and agreed to the published version of the manuscript.

Funding: This work is supported by the Jianghan University School-level Scientific Research Project Funding Program (2022SXZX-ZC-01). The work is also supported by the National Natural Science Foundation of China (52102256 and 51808554).

Institutional Review Board Statement: Not applicable.

Informed Consent Statement: Not applicable.

Data Availability Statement: Not applicable.

Acknowledgments: The authors would like to thank Zhang Qian from Shiyanjia Lab (www.shiyanjia.com, accessed on 15 January 2023) for the SEM analysis.

Conflicts of Interest: The authors declare no conflict of interest.

References

1. Kabra, S.; Gharde, S.; Gore, P.M.; Jain, S.; Khire, V.H.; Kandasubramanian, B. Recent trends in nanothermites: Fabrication, characteristics and applications. *Nano Express* **2020**, *1*, 032001. [CrossRef]
2. Yetter, R.A. Progress towards nanoengineered energetic materials. *Proc. Combust. Inst.* **2020**, *38*, 57–81. [CrossRef]
3. Wang, Y.; Dai, J.; Xu, J.; Shen, Y.; Wang, C.-A.; Ye, Y.; Shen, R. Experimental and numerical investigations of the effect of charge density and scale on the heat transfer behavior of Al/CuO nano-thermite. *Vacuum* **2020**, *184*, 109878. [CrossRef]
4. Wang, C.A.; Xu, J.B.; Shen, Y.; Wang, Y.T.; Yang, T.L.; Zhang, Z.H.; Li, F.; Shen, R.; Ye, Y.H. Thermodynamics and performance of Al/CuO nanothermite with different storage time. *Def. Technol.* **2021**, *17*, 741–747. [CrossRef]
5. Wu, T.; Singh, V.; Julien, B.; Tenailleau, C.; Estève, A.; Rossi, C. Pioneering insights into the superior performance of titanium as a fuel in energetic materials. *Chem. Eng. J.* **2023**, *453*, 139922. [CrossRef]

6. Huang, S.; Hong, S.; Su, Y.; Jiang, Y.; Fukushima, S.; Gill, T.M.; Yilmaz, N.E.D.; Tiwari, S.; Nomura, K.-I.; Kalia, R.K.; et al. Enhancing combustion performance of nano-Al/PVDF composites with β-PVDF. *Combust. Flame* **2020**, *219*, 467–477. [CrossRef]
7. Li, Z.; Wang, N.; Shi, B.; Li, S.; Yang, R. Effects of particle size on two-phase flow loss in aluminized solid rocket motors. *Acta Astronaut.* **2019**, *159*, 33–40. [CrossRef]
8. Cohen, O.; Michaels, D.; Yavor, Y. Agglomeration in Composite Propellants Containing Different Nano-Aluminum Powders. *Propellants Explos. Pyrotech.* **2022**, *47*, e202100320. [CrossRef]
9. Goetz, V.; Gibot, P.; Spitzer, D. Spark sensitivity and light signature mitigation of an Al/SnO2 nanothermite by the controlled addition of a conductive polymer. *Chem. Eng. J.* **2021**, *427*, 131611. [CrossRef]
10. Valluri, S.K.; Schoenitz, M.; Dreizin, E. Fluorine-containing oxidizers for metal fuels in energetic formulations. *Def. Technol.* **2019**, *15*, 1–22. [CrossRef]
11. Yang, H.; Xu, C.; Wang, W.; Tang, P.; Li, X.; He, S.; Bao, H.; Man, S.; Tang, D.; Li, X.; et al. Underwater self-sustaining combustion and micro-propulsion properties of Al@ FAS-17/PTFE-based direct-writing nanothermite. *Chem. Eng. J.* **2023**, *451*, 138720. [CrossRef]
12. Xiong, K.; Zhang, W.; Wang, Y.; Liu, R.; Yang, S.; Nie, H.; Yan, Q.-L. The effects of fluoropolymers with optimized contents on reactivity and combustion behavior of Al/MxOy nanocomposites. *Combust. Flame* **2023**, *249*, 112606. [CrossRef]
13. Uhlenhake, K.E.; Collard, D.N.; Hoganson, A.C.; Brown, A.D.; Fox, S.; Örnek, M.; Rhoads, J.F.; Son, S.F. Additively Manufactured Micro-and Nano-Al/PVDF Ignition Sensitivity and Burning Characterization. *Propellants Explos. Pyrotech.* **2022**, e202200204. [CrossRef]
14. Ke, X.; Guo, S.; Zhang, G.; Zhou, X.; Xiao, L.; Hao, G.; Wang, N.; Jiang, W. Safe preparation, energetic performance and reaction mechanism of corrosion-resistant Al/PVDF nanocomposite films. *J. Mater. Chem. A* **2018**, *6*, 17713–17723. [CrossRef]
15. Wang, H.; Rehwoldt, M.; Kline, D.J.; Wu, T.; Wang, P.; Zachariah, M.R. Comparison study of the ignition and combustion characteristics of directly-written Al/PVDF, Al/Viton and Al/THV composites. *Combust. Flame* **2018**, *201*, 181–186. [CrossRef]
16. Du, J.; Li, J.; Zhang, Z.Y.; Yang, G.; Li, Y.; Wei, J.Z. Study on influence factors of the combustion temperature of MTV foil-type decoys and their interactions. *Sci. Technol. Energetic Mater.* **2019**, *80*, 99–106.
17. Koch, E.C.; Hahma, A. Metal-fluorocarbon pyrolants. XIV: High density-high performance decoy flare compositions based on ytterbium/polytetrafluoroethylene/viton®. *Z. Für Anorg. Und Allg. Chem.* **2012**, *638*, 721–724. [CrossRef]
18. Feng, B.; Qiu, C.L.; Zhang, T.H.; Hu, Y.F.; Li, H.G.; Xu, B.C. Sensitivity of Al-PTFE upon Low-Speed Impact. *Propellants Explos. Pyrotech.* **2019**, *44*, 630–636. [CrossRef]
19. Tang, L.; Wang, H.; Lu, G.; Zhang, H.; Ge, C. Mesoscale study on the shock response and initiation behavior of Al-PTFE granular composites. *Mater. Des.* **2021**, *200*, 109446. [CrossRef]
20. Uhlenhake, K.E.; Yehia, O.R.; Noel, A.; Terry, B.C.; Örnek, M.; Belal, H.M.; Gunduz, I.E.; Son, S.F. On the Use of Fluorine-Containing Nano-Aluminum Composite Particles to Tailor Composite Solid Rocket Propellants. *Propellants Explos. Pyrotech.* **2022**, *47*, e202100370. [CrossRef]
21. Chen, S.; Yu, H.; Zhang, W.; Shen, R.; Guo, W.; DeLuca, L.T.; Wang, H.; Ye, Y. Sponge-like Al/PVDF films with laser sensitivity and high combustion performance prepared by rapid phase inversion. *Chem. Eng. J.* **2020**, *396*, 124962. [CrossRef]
22. Wang, H.; Shen, J.; Kline, D.J.; Eckman, N.; Agrawal, N.R.; Wu, T.; Wang, P.; Zachariah, M.R. Direct Writing of a 90 wt% Particle Loading Nanothermite. *Adv. Mater.* **2019**, *31*, e1806575. [CrossRef] [PubMed]
23. Sevely, F.; Liu, X.; Wu, T.; Mesnilgrente, F.; Franc, B.; Assie-Souleille, S.; Dollat, X.; Rossi, C. Effect of Process Parameters on the Properties of Direct Written Gas-Generating Reactive Layers. *ACS Appl. Polym. Mater.* **2021**, *3*, 3972–3980. [CrossRef]
24. Shen, J.; Wang, H.; Kline, D.J.; Yang, Y.; Wang, X.; Rehwoldt, M.; Wu, T.; Holdren, S.; Zachariah, M.R. Combustion of 3D printed 90 wt% loading reinforced nanothermite. *Combust. Flame* **2020**, *215*, 86–92. [CrossRef]
25. Zhang, D.; Li, X. Fabrication and kinetics study of nano-Al/NiO thermite film by electrophoretic deposition. *J. Phys. Chem. A* **2015**, *119*, 4688–4694. [CrossRef]
26. Dulmaa, A.; Depla, D. Influence of Impurities on the Front Velocity of Sputter Deposited Al/CuO Thermite Multilayers. *Materials* **2021**, *14*, 7224. [CrossRef]
27. Wang, H.; Biswas, P.; Kline, D.J.; Zachariah, M.R. Flame stand-off effects on propagation of 3D printed 94 wt% nanosized pyrolants loading composites. *Chem. Eng. J.* **2022**, *434*, 134487. [CrossRef]
28. Mao, Y.; Zhong, L.; Zhou, X.; Zheng, D.; Zhang, X.; Duan, T.; Nie, F.; Gao, B.; Wang, D. 3D Printing of Micro-Architected Al/CuO-Based Nanothermite for Enhanced Combustion Performance. *Adv. Eng. Mater.* **2019**, *21*, 1900825. [CrossRef]
29. Zhong, L.; Zhou, X.; Huang, X.; Zheng, D.; Mao, Y.; Wang, R.; Wang, D. Combustion/decomposition characteristics of 3D-printed Al/CuO, Al/Fe2O3, Al/Bi2O3 and Al/PTFE hollow filaments. *Mater. Chem. Phys.* **2021**, *271*, 124874. [CrossRef]
30. Murray, A.K.; Novotny, W.A.; Fleck, T.J.; Gunduz, I.E.; Son, S.F.; Chiu, G.; Rhoads, J.F. Selectively-deposited energetic materials: A feasibility study of the piezoelectric inkjet printing of nanothermites. *Addit. Manuf.* **2018**, *22*, 69–74. [CrossRef]
31. Wang, H.; Holdren, S.; Zachariah, M.R. Preparation and combustion of laminated iodine containing aluminum/polyvinylidene fluoride composites. *Combust. Flame* **2018**, *197*, 120–126. [CrossRef]
32. Yang, H.; Huang, C.; Chen, H. Tuning reactivity of nanoaluminum with fluoropolymer via electrospray deposition. *J. Therm. Anal. Calorim.* **2016**, *127*, 2293–2299. [CrossRef]
33. Lyu, J.-Y.; Chen, S.; He, W.; Zhang, X.-X.; Tang, D.-Y.; Liu, P.-J.; Yan, Q.-L. Fabrication of high-performance graphene oxide doped PVDF/CuO/Al nanocomposites via electrospinning. *Chem. Eng. J.* **2019**, *368*, 129–137. [CrossRef]

34. Huang, S.; Pan, M.; Deng, S.; Jiang, Y.; Zhao, J.; Levy-Wendt, B.; Tang, S.K.; Zheng, X. Modified Micro-Emulsion Synthesis of Highly Dispersed Al/PVDF Composites with Enhanced Combustion Properties. *Adv. Eng. Mater.* **2019**, *21*, 1801330. [CrossRef]
35. Rehwoldt, M.C.; Wang, H.; Kline, D.J.; Wu, T.; Eckman, N.; Wang, P.; Agrawal, N.R.; Zachariah, M.R. Ignition and combustion analysis of direct write fabricated aluminum/metal oxide/PVDF films. *Combust. Flame* **2019**, *211*, 260–269. [CrossRef]
36. Zheng, S.; Yang, Y.; Li, X.; Liu, H.; Yan, W.; Sui, R.; Lu, Q. Temperature and emissivity measurements from combustion of pine wood, rice husk and fir wood using flame emission spectrum. *Fuel Process. Technol.* **2020**, *204*, 106423. [CrossRef]
37. Nie, H.; Tan, L.P.; Pisharath, S.; Hng, H.H. Nanothermite composites with a novel cast curable fluoropolymer. *Chem. Eng. J.* **2021**, *414*, 128786. [CrossRef]
38. Weismiller, M.; Lee, J.; Yetter, R. Temperature measurements of Al containing nano-thermite reactions using multi-wavelength pyrometry. *Proc. Combust. Inst.* **2011**, *33*, 1933–1940. [CrossRef]
39. Huang, C.; Jian, G.; DeLisio, J.B.; Wang, H.; Zachariah, M.R. Electrospray Deposition of Energetic Polymer Nanocomposites with High Mass Particle Loadings: A Prelude to 3D Printing of Rocket Motors. *Adv. Eng. Mater.* **2014**, *17*, 95–101. [CrossRef]
40. Bencomo, J.A.; Iacono, S.T.; McCollum, J. 3D printing multifunctional fluorinated nanocomposites: Tuning electroactivity, rheology and chemical reactivity. *J. Mater. Chem. A* **2018**, *6*, 12308–12315. [CrossRef]
41. McCollum, J.; Morey, A.M.; Iacono, S.T. Morphological and combustion study of interface effects in aluminum-poly (vinylidene fluoride) composites. *Mater. Des.* **2017**, *134*, 64–70. [CrossRef]